

# tc-2020-147 Reviewer 1 Response

Huw Horgan et al

August 2020

The reviewer raises some useful points that highlight the need for clarification, additional work, and a wider ranging introduction and discussion. We address these below. The reviewer's comments are shown in italics and our replies are shown in plain text.

*The authors present an active seismic study in the grounding zone of the Whillans Ice Stream. Although their seismic methods are interesting, the paper needs a lot of work. Basic hypotheses (i.e., the influence of tides) about their findings are unexplored. Their clustering analysis is threadbare. Most lacking is the intellectual context. Other groups (besides folks from Penn State) do work on Whillans and it would benefit progress in the field if the authors showed more interest in interacting with these other lines of inquiry. Despite these criticisms, I do think that a significantly modified manuscript could meet publication standards in the Cryosphere.*

*Data, Methods, Results*

## 1 Clustering

*First major point: the clustering warrants more detail. How was the number of clusters chosen? It would be useful to see an L-curve analysis to persuade the reader that three is a reasonable number. Were error bounds included in the cluster analysis? It would be interesting to do so. It would also be interesting to see the clustering carried out with Vs included for the following reason. A reasonable null hypothesis would be that there exist two clusters: grounded and floating. These two clusters should be mainly distinguished by Vs. Perhaps the results indicate that grounding zone is more complicated than this simple picture? 2D scatter plots of the clustering results should be shown to demonstrate the validity of the underlying method. See <https://scikit-learn.org/stable/modules/clustering.html>. Different clustering methods work well with different structures in the data and it's not clear that K-Means is the right choice for this application.*

The clustering we perform is not a central part of our result but this is a good point. Our intent was to see if our results separated into floating, grounded, and

other values. This was primarily to enable reporting of representative values for the grounded and floating portions but we also hoped to highlight where the grounded portion of the ice stream exhibited properties suggestive of subglacial water. Following the advice of the reviewer we have explored this further. The reviewer’s suggestion to use the scikit-learn module proved useful for this analysis. The reviewer’s comment that we needed to demonstrate the suitability of the kmeans method, and the chosen number of clusters is well founded. The null hypothesis that  $V_s$  should be used to discriminate makes sense, except for the fact that we are not as skilful a recovering  $V_s$  as we are at recovering  $R_b$ ,  $V_p$  or  $\rho$ .

### 1.1 Kmeans clustering

We first present our original analysis using Kmeans and  $V_p$ ,  $R_b$  and  $\rho$  (Figure 1). We have now included our uncertainties in the analysis and have seeded the initial positions with 100 random starting points. To assess the chosen number of clusters we have followed the reviewer’s advice and examined the inertia values for different numbers of clusters (Figure 1A) and scatter plots of the optimal number of clusters (Figure 1C). Figure 1A indicates 3 clusters is appropriate. While the clusters clearly delineate the grounding zone (9000 m in Figure 1B) the scatter plots show that the data structures are anisotropic some clusters cuts across data structures (Figure 1C).

We then perform Kmeans clustering based on  $V_s$  values as suggested. This results in the inertia curve shown in Figure 2A, which indicates three clusters is most appropriate. Clustering into two groups results in Figure 2B,C and three groups results in Figure 3. Figure 2B shows that a two cluster analysis results in clusters that are not well spatially defined and Figure 2C shows clusters cut across data structures. Three clusters (Figure 3) results in a similar mixing of clusters above and below the grounding line and clusters that cut across data structures.

Instead of using  $V_s$ , we suggest that clustering of normal incidence reflection coefficient  $R_b$  values is appropriate.  $R_b$  values should clearly distinguish water at the base of the ice, which should exhibit high amplitude negative values.  $R_b$  values are also obtained independent of the non linear inversion of the Zoeppritz equations and thus provide a useful check of the methodology. The inertia plot of  $R_b$  values indicates three clusters in most appropriate. We present the results of a two cluster analysis (Figure 4) and three cluster analysis (Figure 5). The two cluster analysis results in clusters almost entirely separated by the grounding line (Figure 4B). Scatter plots (Figure 4C) show the clusters do not cut across data structures. Three clusters (Figure 5) results in the floating portion of the profile separating into two cluster (Figure 5A) with two values upstream of the grounding line grouping with values from the floating portion. Scatter plots (Figure 5B) show clusters that in places cut across data structures.

We also investigated Kmeans clustering of  $V_s$  and  $V_p$  values (Figure 6) as high ratios of  $V_p$  to  $V_s$  should be a strong indicator of the presence of liquid. The inertia plot (Figure 6) indicates a two cluster analysis is most appropri-

ate. This results in a spatial mixing of clusters above and below the grounding zone (Figure 6B), likely due to the poorly constrained  $V_s$  values. Scatter plots (Figure 6C) show the clusters cut across  $\rho-V_p$  data structures.

## 1.2 DBSCAN clustering

Due to a concern that clustering with the Kmeans algorithm may be unsuitable due to the shape and anisotropy of our clusters we investigated clustering using the DBSCAN algorithm (Ester et al., 1996). DBSCAN clusters are based on data density and the technique is relatively insensitive to outliers. DBSCAN does not require the number of clusters to be predetermined but is sensitive to a distance parameter (eps) used to define clusters and a minimum number of points used to define a cluster is also predefined. We present results with eps values determined using the nearest neighbor sorted distance method. Here we present DBSCAN clustering of  $R_b$  (Figure 7),  $V_s$  (Figure 8), and  $V_s$  and  $V_p$  (Figures 9– 10).

DBSCAN clustering of  $R_b$  values is presented in Figure 7. The sorted near neighbor distance curve and the resulting number of clusters and noise points produced by a range of eps values and minimum number of samples is shown in Figure 7A. The elbow of the sorted distance curve indicates an eps value of around 0.05 is appropriate. However, we apply an eps=0.075 as values less than this result in either too many clusters or too many noise points. Even with eps=0.075 and the minimum number of points set to 4, DBSCAN results in 8 clusters and identifies 30 noise points (Figure 7B,C). These clusters group above and below the grounding zone (Figure 7B) and cut across data structures (Figure 7C).

DBSCAN clustering of  $V_s$  values (Figure 8) indicates an eps setting of 0.05 is appropriate (Figure 8A). Combined with a minimum number of points set to 4, this results in 14 clusters with 6 noise points identified (Figure 8B,C). These clusters cut across the grounding line (Figure 8B) and across data structures (Figure 8C).

DBSCAN clustering of  $V_s$  and  $V_p$  values results in a near neighbor curve indicating an eps value of approximately 0.2 (Figure 9A). The steps in the near neighbor curve result from the variable data density. An eps set to 0.2 requires a low number of minimum points (Figure 9A), which we set to 3. This results in 7 clusters and 36 points identified as noise, with almost all the noise points located above the grounding zone (Figure 9B). Increasing the eps setting to 0.475 and increasing the minimum number of points to 4 results in just 3 clusters, which are largely separated by the grounding line (Figure 10A), and 7 noise points. Scatter plots (Figure 10B) show the clusters generally don't cut across data structures. This eps setting is, however, not justified by the near neighbor distance plot.

### 1.3 Conclusion

Both clustering approaches we have explored are not well suited to our intended purpose. Reasonable results can be obtained with either Kmeans using our previous parameters, or a Kmeans 2 cluster analysis of  $R_b$ . DBSCAN requires us to use higher eps values than suggested by our near neighbour analysis to obtain a useful number of clusters and noise points. The Kmeans method is likely sensitive to the anisotropy in our data, while the DBSCAN method is likely to be susceptible to the varying levels of data density. As we are primarily interested in grouping above and below the grounding zone and reporting representative values we suggest the following.

- Present the repeat kinematic GNSS analysis of the grounding zone (see next section).
- Report the mode bin values after binning of the results at an appropriate resolution.
- Archive full results with a DOI so interested parties can group or recalculate as they wish.

## 2 Tidal influence

*Second major point: Were the shots all fired at the same phase of the tides? See the work by Victor Tsai and others about tidal grounding line migration. Perhaps this is why Line 1 appears to have not hit the ocean cavity? Perhaps the ice was in contact with ocean sediments during the time of acquisition.*

### 2.1 Timing of shots

The shots were not fired at the same phase of the tide. This would not be feasible for an experiment of this scale. Figure 11 shows the timing of the shots and the tidal elevation both as a function of time, and as a function of distance along the profiles. We are unclear what the reviewer means by *Perhaps this is why Line 1 appears to have not hit the ocean cavity?* as Line 1 did hit the ocean cavity which is imaged from approximately Kilometer 9 until the end of the profile. We hope that our inclusion of Figure 12 clarifies this and we will now explicitly label the ocean cavity in the seismic profiles. Figure 11A shows that Kilometer 6–12.5 of Line 1 was acquired on the falling tide when the tidal elevation varied from +0.1 m to -0.6 m. The pronounced change in basal reflectivity that occurs at approximately Kilometer 9 on Line 1 does not coincide with a step in the tidal elevation. Other step-changes in tidal elevation along Line 1 also do not coincide with changes in basal reflectivity (e.g. Kilometer 1). Lines 2–4 all took less than a day to acquire and have no major step-changes in tidal elevation along the profiles. The onset of high basal reflectivity in Line 2 occurs in proximity to a 0.3 m change in tidal elevation offshore, however, repeat kinematic profiling (Figure 12) indicates vertical change at this location

is likely to be much less and even a 0.3 m change in water column thickness would be insufficient to cause the change in reflectivity observed.

## 2.2 Tidal grounding line migration – Repeat GNSS transects across the grounding zone.

Figure 12 shows repeat kinematic profiling along Lines 1 and 2. These repeat kinematic profiles were acquired at the times shown in the right hand panels in the figure. We have previously used these data to validate a seismically determined grounding line location (Horgan et al., 2013). We locate the grounding zone using the standard deviation in 50 m spatial bins. Upstream of the grounding zone we expect this value to represent the method uncertainty (both the GNSS observations, and our ability to repeat a track precisely) combined with a measure of the roughness of the surface. Downstream these combine with the displacement of the ice surface due to the tide. The grounding line is determined to be the point at which the standard deviation changes from values representative of grounded upstream values to those representative of floating values. The pick is subject to some interpretation as roughness varies spatially and can correlate with surface slope.

Both lines were measured using kinematic GNSS on the rising tide. The tidal range for Line 1 at the time we observed was approximately 1.5 m, while Line 2 we observed a smaller range of approximately 0.35 m. Both profiles exhibit a region of relatively-high surface slope that begins upstream of the onset of vertical tidal displacement. This zone of relatively high surface slope is observed at the grounding zone of much of the Siple and Gould Coasts (Horgan and Anandakrishnan, 2006). We pick the Line 1 grounding zone at Kilometer 9.6 for Line 1, and Kilometer 3.6 for Line 2. Well upstream of the grounding zone (>4 km) our repeat tracks typically all fall within 0.1 m vertically of each other. At the resolution of our data we do not observe migration of the grounding line in the GNSS data, nor do we observe any spatial patterns in basal reflectivity that could be attributed to tidal variation given the wavelength of our seismic source is nominally approximately 14 m in water.

## 2.3 Conclusion

In our submission we referenced earlier work that determined the grounding zone location using repeat kinematic GNSS profiling. We now see that reproducing those data here and in the manuscript would be beneficial and add clarity. We will also present the experiment timing and tide model results.

## 3 Other points

*Other points: It would be useful to also report  $Q$  values. Figure 4 (and elsewhere), What are the units of source size? What is the symbol  $R_b$ ? The text*

only defines  $R_{bInt}$  and  $R_{b10}$ . Table 4. Does the plus/minus range indicate one standard deviation?

We can present Q values for representative frequencies. The units of source size are the same as amplitude (counts).  $R_b$  is normal incidence basal reflectivity and  $R_{bInt}$  and  $R_{b10}$  are two common ways of calculating it. The plus/minus range indicates one standard deviation.

## 4 Discussion, Conclusions

*\*\*Discussion, Conclusions\*\* I found the discussion to be quite narrow. Whillans is a complex, interesting, and unusual system. The ice stream is decelerating and is expected to be a major stabilizer of Antarctic ice loss. Yet when we go to probe the nature of the deceleration, we see that ice flow is quite bizarre and exhibits a remarkable large scale stick-slip motion. Despite this fascinating situation, the most that the authors can offer in terms of the implications for ice flow is the already-established point that "The rapid transition in basal properties indicates that the full Stokes equations are likely to be needed to be solved if the ice flow velocity field is to be accurately." The authors also mention the Walker 2013 paper. As written, this paper could be submitted to a seismology-focused journal like BSSA. As indicated in the next section of the review, it would be nicer to see closer integration with other lines of inquiry.*

*\*\*References\*\* 27 out of 49 of the citations in this paper are to the Penn State group. Of the other 22 citations, the average citation age is in the mid 1990's and none are about the Whillans Ice Stream. I'm surprised to see no mention of any of the numerous modeling studies that have been carried out on Whillans:*

- Bougamont, Marion, Slawek Tulaczyk, and Ian Joughin. "Numerical investigations of the slow-down of Whillans Ice Stream, West Antarctica: is it shutting down like IceStream C?" *Annals of Glaciology* 37 (2003): 239-246.
- Goldberg, D., C. Schoof, and O. Sergienko (2014), Stick-slip motion of an Antarctic icestream: The effects of viscoelasticity, *J. Geophys. Res. Earth Surf.*, 119, 1564–1580, doi:10.1002/2014JF003132.
- Lipovsky, B. P., and E. M. Dunham (2017), Slow-slip events on the Whillans Ice Plain, Antarctica, described using rate-and-state friction as an ice stream sliding law, *J. Geophys. Res. Earth Surf.*, 122, doi:10.1002/2016JF004183.
- Sergienko, O. V., D. R. MacAyeal, and R. A. Bindschadler (2009), Stick-slip behavior of ice streams: Modeling investigations, *Ann. Glaciol.*, 50(52), 87–94.

*Similarly for the observational studies of other groups,*

- *Beem, L. H., et al. "Variable deceleration of Whillans Ice Stream, West Antarctica." *C3Journal of Geophysical Research: Earth Surface* 119.2 (2014): 212-224.*
- *Stearns, Leigh A., Kenneth C. Jezek, and Cornelis J. Van Der Veen. "Decadal-scale variations in ice flow along Whillans Ice Stream and its tributaries, West Antarctica." *Journal of Glaciology* 51.172 (2005): 147-157.*
- *Walter, J. I., E. E. Brodsky, S. Tulaczyk, S. Y. Schwartz, and R. Pettersson (2011), Transient slip events from near-field seismic and geodetic data on a glacier fault, Whillans Ice Plain, West Antarctica, *J. Geophys.Res.*, 116, F01021, doi:10.1029/2010JF001754.*

*Other shelf/stream papers besides the Penn State Walker et al 2013 paper:*

- *Tsai, Victor C., and G. Hilmar Gudmundsson. "An improved model for tidally modulated grounding-line migration." *Journal of Glaciology* 61.226 (2015): 216-222.*
- *Sayag, R., and M. Grae Worster. "Elastic dynamics and tidal migration of grounding lines modify subglacial lubrication and melting." *Geophysical research letters* 40.22(2013): 5877-5881.*

*Finally, it is somewhat glaring that there are no citations to the WISSARD project on the Whillans Ice Stream. The authors mention basal "ponding". Other grounds call these ponds subglacial lakes:*

- *Tulaczyk, Slawek, et al. "WISSARD at Subglacial Lake Whillans, West Antarctica: scientific operations and initial observations." *Annals of Glaciology* 55.65 (2014): 51-58.*
- *Carter, S. P., H. A. Fricker, and M. R. Siegfried. "Evidence of rapid subglacial water piracy under Whillans Ice Stream, West Antarctica." *Journal of Glaciology* 59.218(2013): 1147-1162.*
- *Siegfried, Matthew R., et al. "A decade of West Antarctic subglacial lake interactions from combined ICESat and CryoSatR2 altimetry." *Geophysical Research Letters* C4 41.3 (2014): 891-898.*

*Note that I'm not saying the authors need to cite every one of these papers. Rather, it would simply be nice to see a little bit more interaction with the rest of the intellectual community on topics of interest.*

Our referencing reflects the methodological focus of our contribution (over-snow seismic surveying is a relatively rare method) and an ongoing body of work examining the grounding zone of Whillans Ice Stream. That said, our enthusiasm for the method has admittedly resulted in a somewhat myopic focus. We welcome the opportunity to incorporate our findings into the wider literature addressing grounding zone processes and the flow of Whillans Ice Stream. In

particular the work of Tsai and Gudmundsson, and Sayag and Worster are highly relevant and should be discussed in parallel with the study of Walker et al in both the introduction and discussion. A wider ranging discussion of the distribution of water beneath Whillans Ice Stream and associated phenomena is also appropriate.



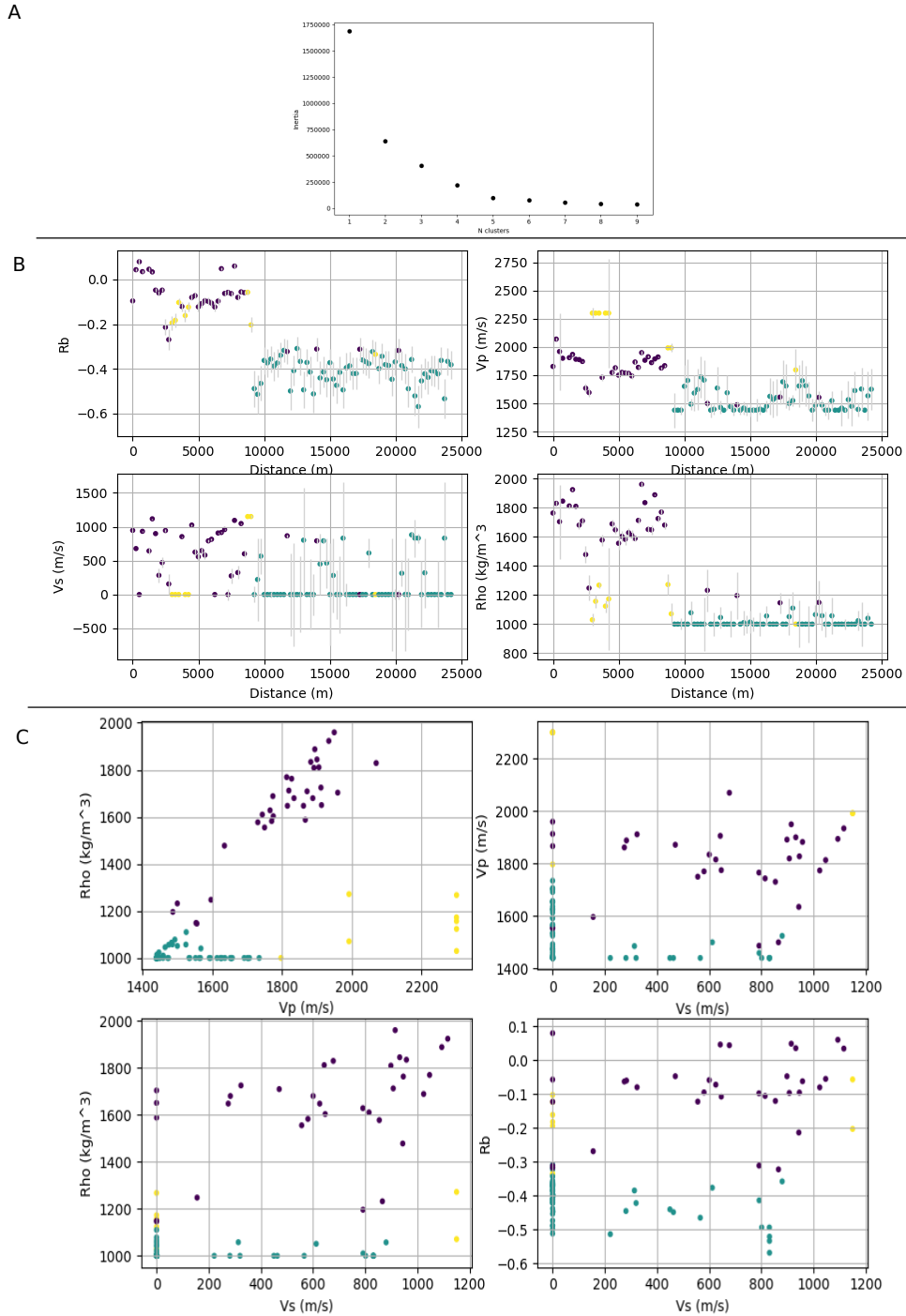


Figure 1: Result of Kmeans clustering of  $R_b$ ,  $V_p$ , and  $\rho$  values. A) Number of Kmeans clusters (x-axis) plotted against inertia. B) Spatial distribution of seismic parameters coloured by cluster for 3 clusters. C) Scatter plots of recovered seismic parameters coloured by cluster for 3 clusters.

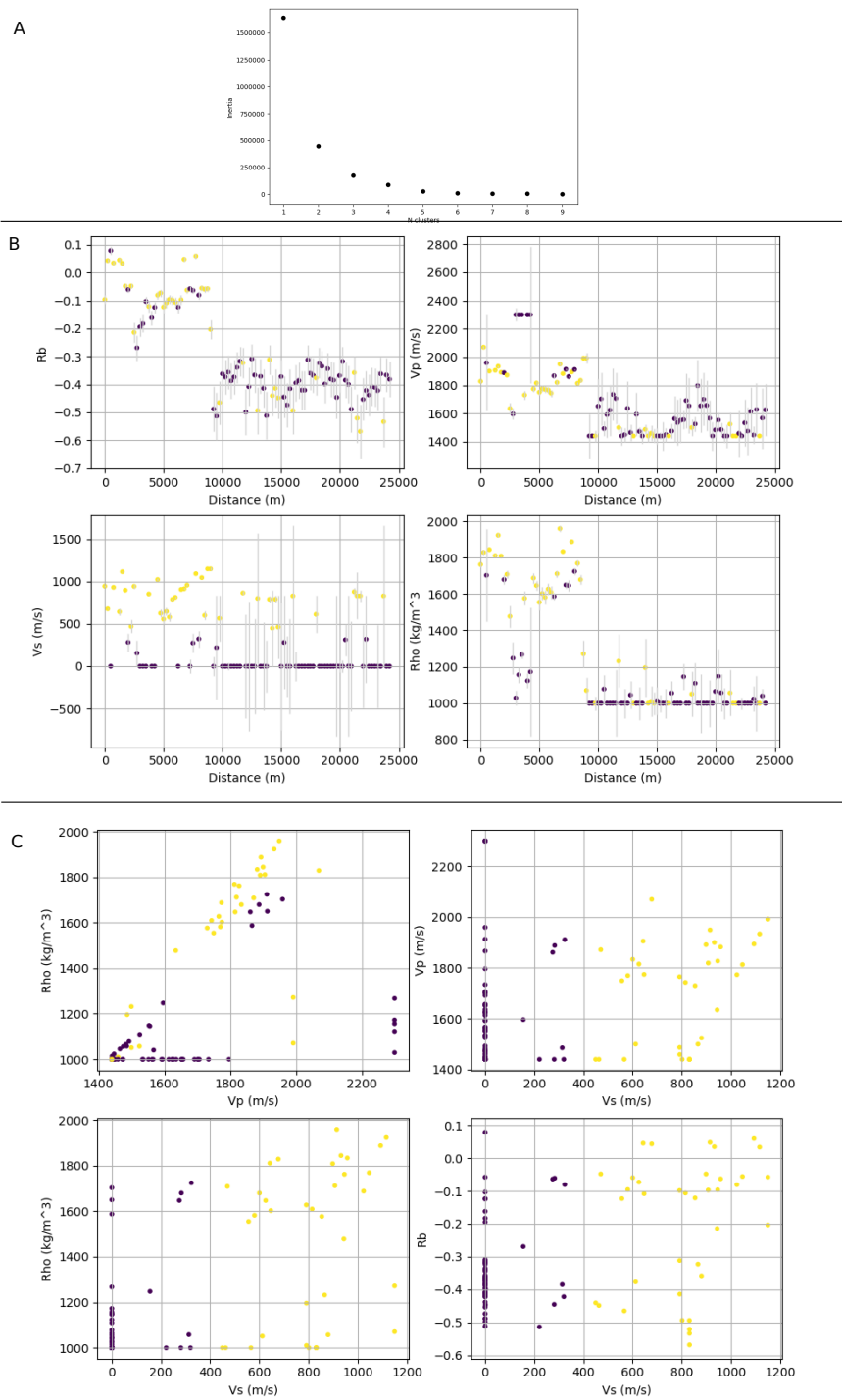


Figure 2: Result of Kmeans clustering of  $V_s$  values. A) Number of Kmeans clusters (x-axis) plotted against inertia. B) Spatial distribution of seismic parameters coloured by cluster for 2 clusters. C) Scatter plots of recovered seismic parameters coloured by cluster for 2 clusters.

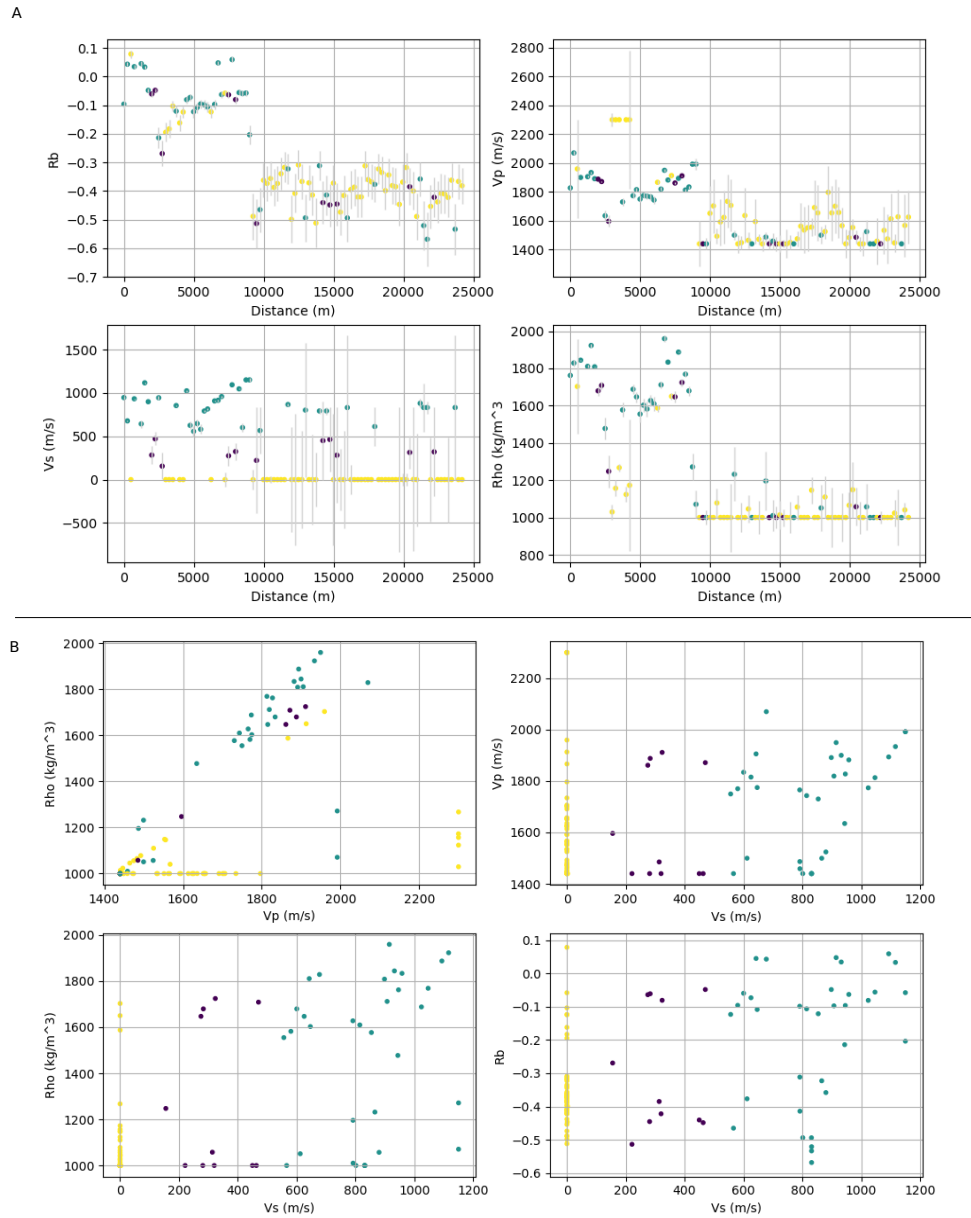


Figure 3: Result of Kmeans clustering of  $V_s$  values. A) Spatial distribution of seismic parameters coloured by cluster for 3 clusters. B) Scatter plots of recovered seismic parameters coloured by cluster for 3 clusters.

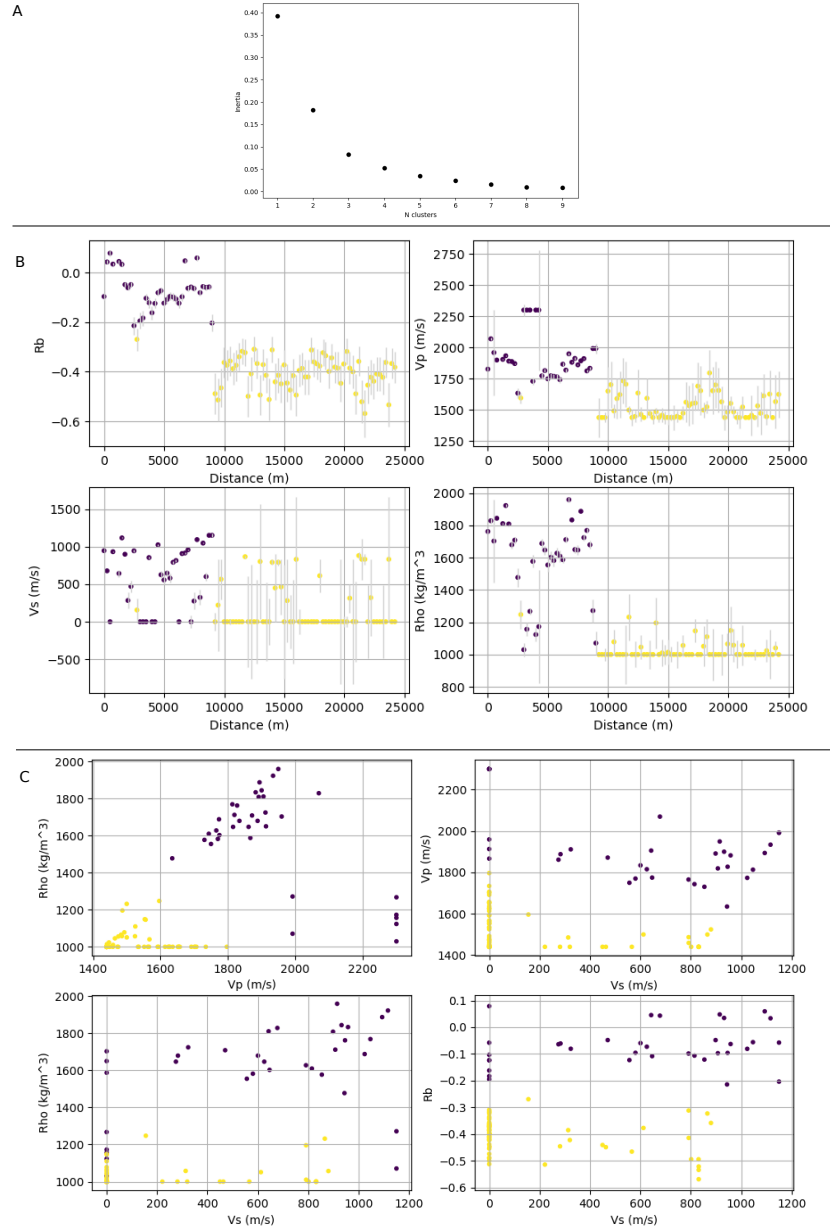


Figure 4: Result of Kmeans clustering of  $R_b$  values. A) Number of Kmeans clusters (x-axis) plotted against inertia. B) Spatial distribution of seismic parameters coloured by cluster for 2 clusters. C) Scatter plots of recovered seismic parameters coloured by cluster for 2 clusters.

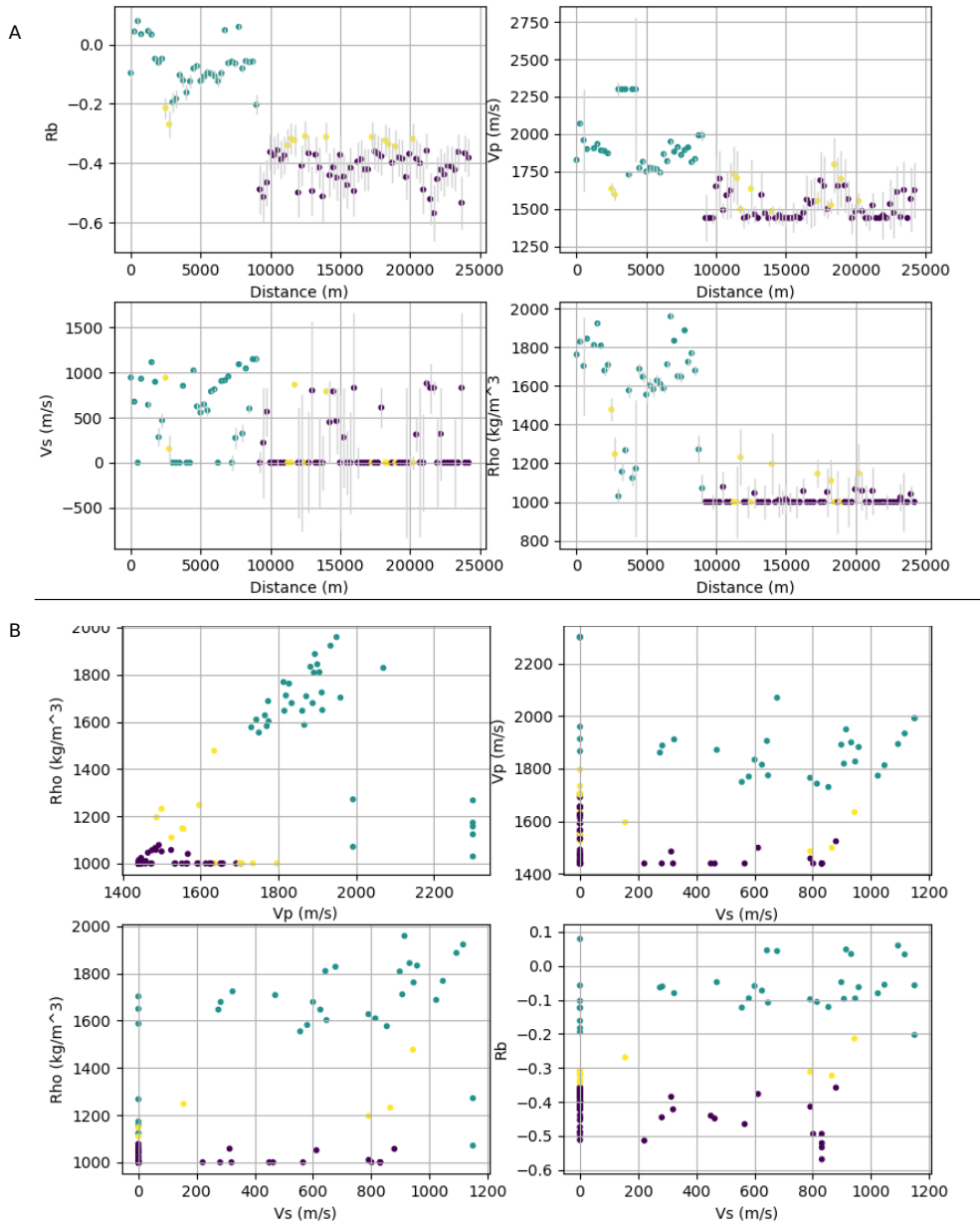


Figure 5: Result of Kmeans clustering of  $R_b$  values. A) Spatial distribution of seismic parameters coloured by cluster for 3 clusters. B) Scatter plots of recovered seismic parameters coloured by cluster for 3 clusters.

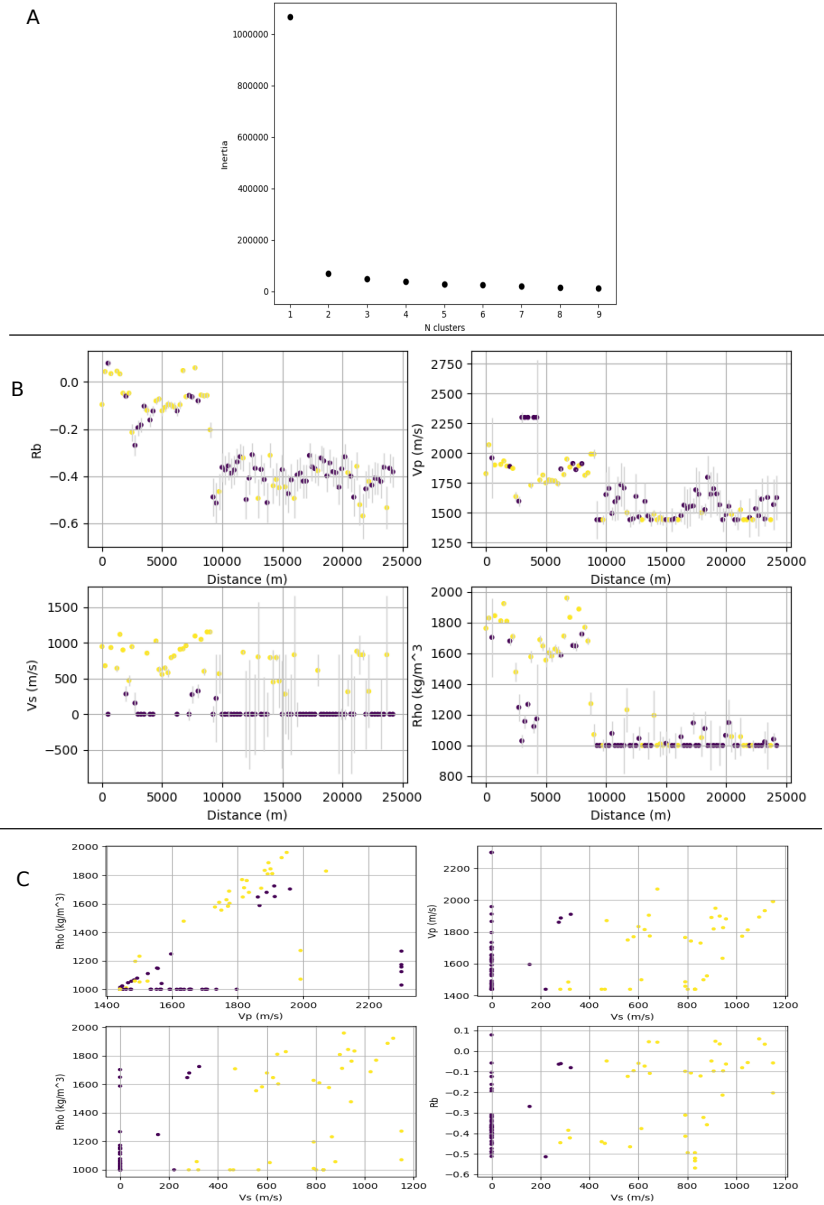


Figure 6: Result of Kmeans clustering of  $V_s$  and  $V_p$  values. A) Number of Kmeans clusters (x-axis) plotted against inertia. B) Spatial distribution of seismic parameters coloured by cluster for 2 clusters. C) Scatter plots of recovered seismic parameters coloured by cluster for 2 clusters.

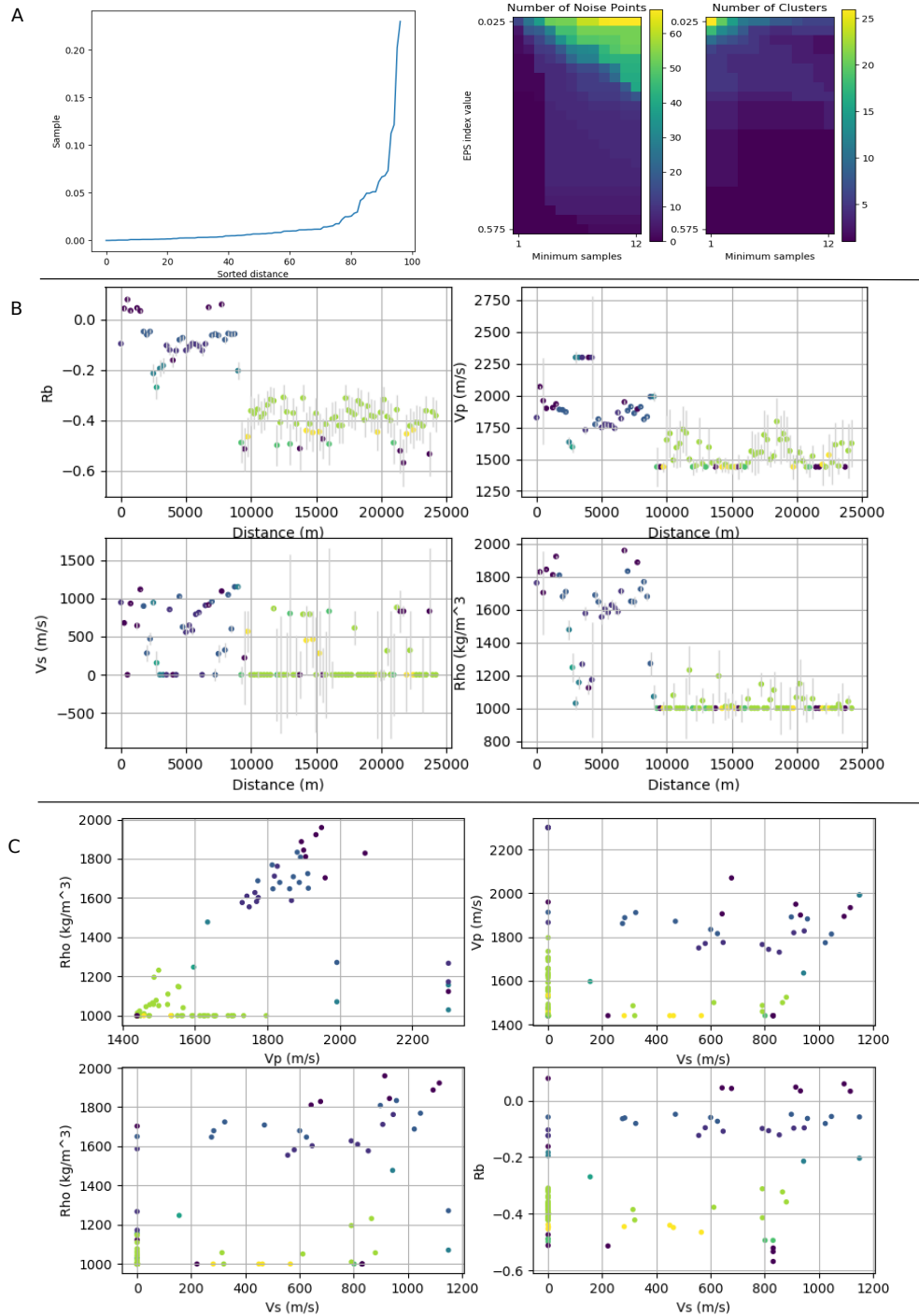


Figure 7: DBSCAN clustering of  $R_b$  values. A) Left: Sorted near neighbour distances. Right: Resulting Number of noise points and number of clusters for a range of eps and minimum sample values. B) Spatial distribution seismic properties coloured by clusters for Line 1. Clustering used eps=0.075 and a minimum number of samples = 3. Noise points shown in black. C) Scatter plots of retrieved seismic values colored by cluster.

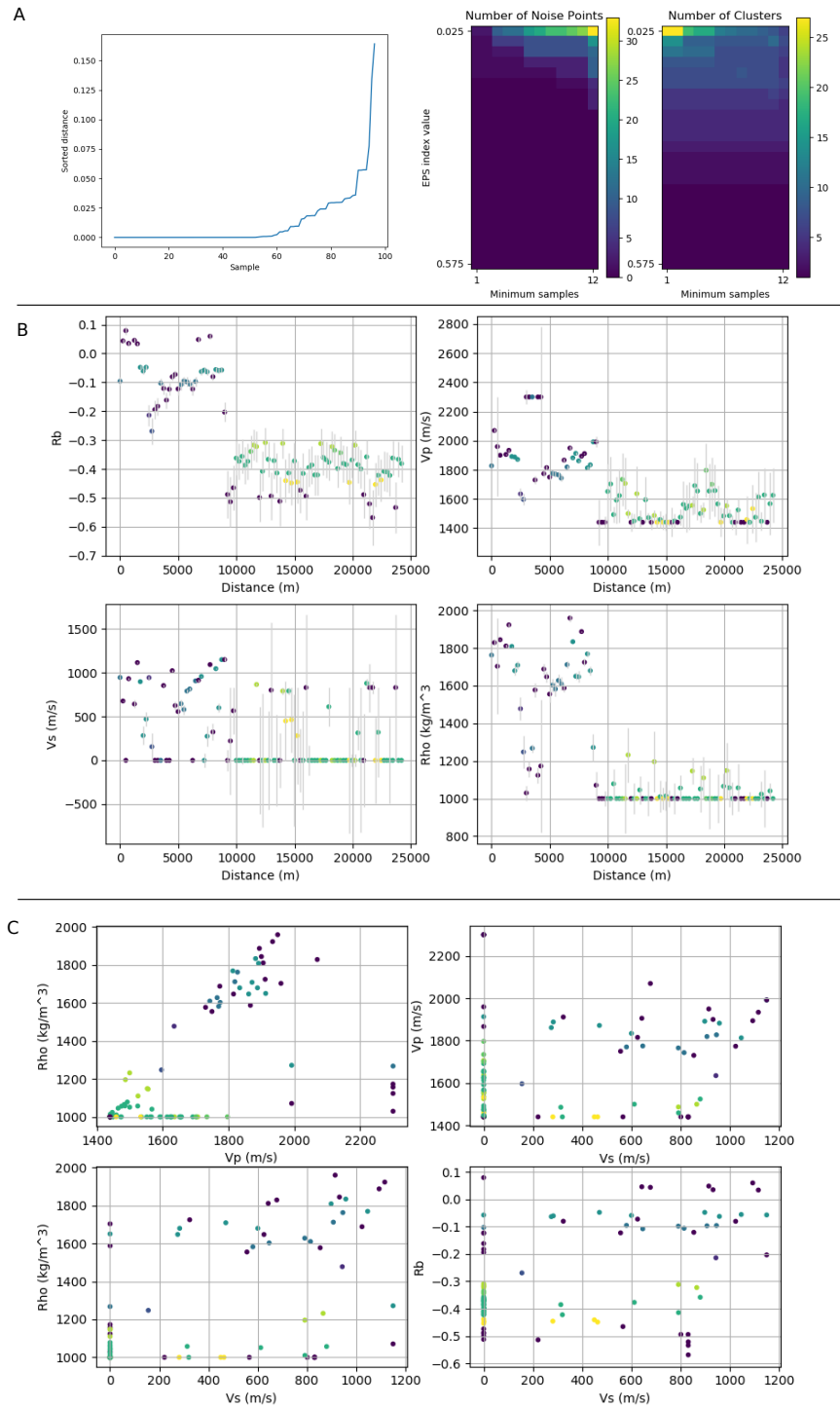


Figure 8: DBSCAN clustering of  $V_s$  values. A) Left: Sorted near neighbour distances. Right: Resulting Number of noise points and number of clusters for a range of eps and minimum sample values. B) Spatial distribution seismic properties coloured by clusters for Line 1. Clustering used eps=0.05 and a minimum number of samples = 4. Noise points shown in black. C) Scatter plots of retrieved seismic values colored by cluster.



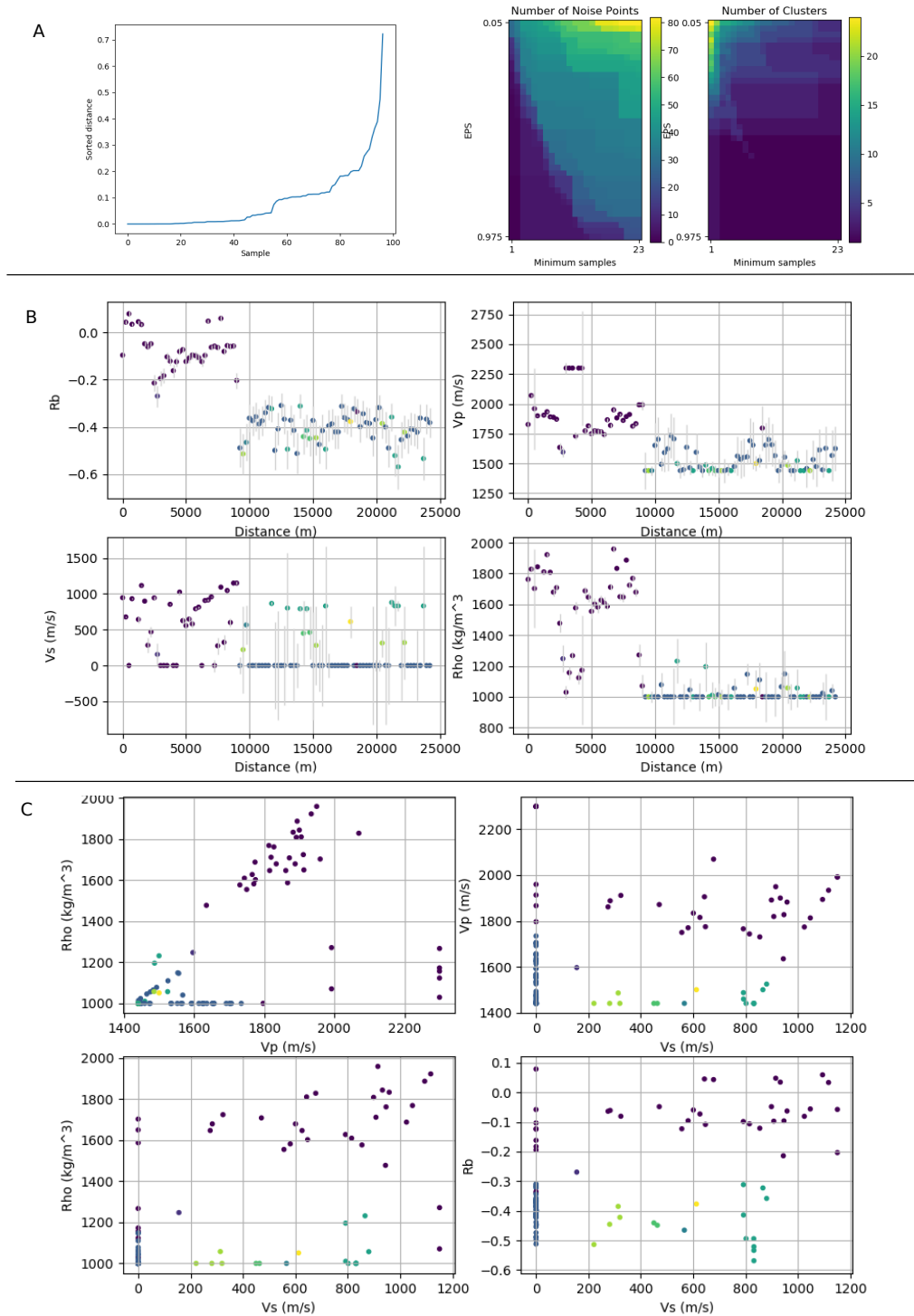
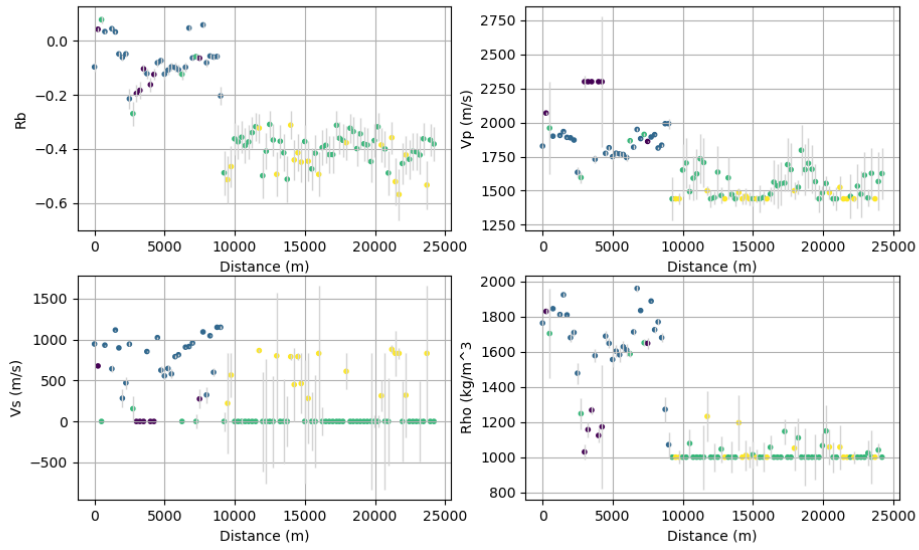


Figure 9: DBSCAN clustering of  $V_s$  and  $V_p$  values. A) Left: Sorted near neighbour distances. Right: Resulting Number of noise points and number of clusters for a range of eps and minimum sample values. B) Spatial distribution seismic properties coloured by clusters for Line 1. Clustering used eps=0.2 and a minimum number of samples = 3. Noise points shown in black. C) Scatter plots of retrieved seismic values colored by cluster.

A



B

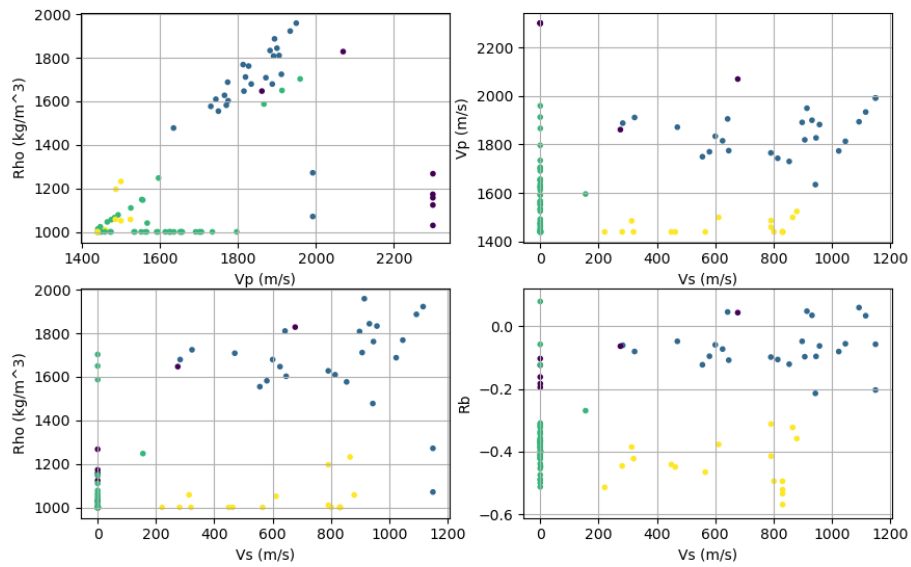


Figure 10: DBSCAN clustering of  $V_s$  and  $V_p$  values. A) Spatial distribution seismic properties coloured by clusters for Line 1. Clustering used  $\text{eps}=0.475$  and a minimum number of samples = 4. Noise points shown in black. B) Scatter plots of retrieved seismic values colored by cluster.

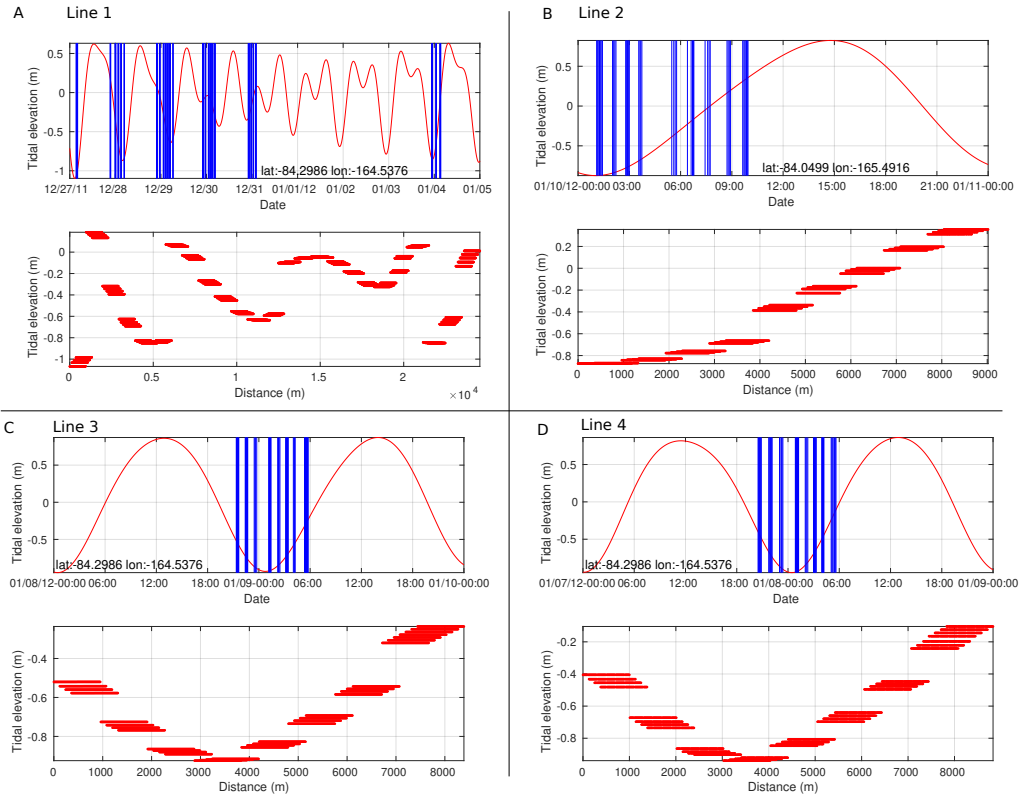


Figure 11: Shot timing and vertical tidal elevation. A) Line 1. Top subplot shows the timing of shots (blue bars) overlain on the vertical tidal elevation from Tide Model Driver (Pandman and Erofeeva (2005)). Bottom subplot shows the Tide Model Driver (Padman and Erofeeva, 2005) elevation at the time of shooting as a function of distance along the profile. B-C) same as A) but for lines 2, 3, and 4, respectively.

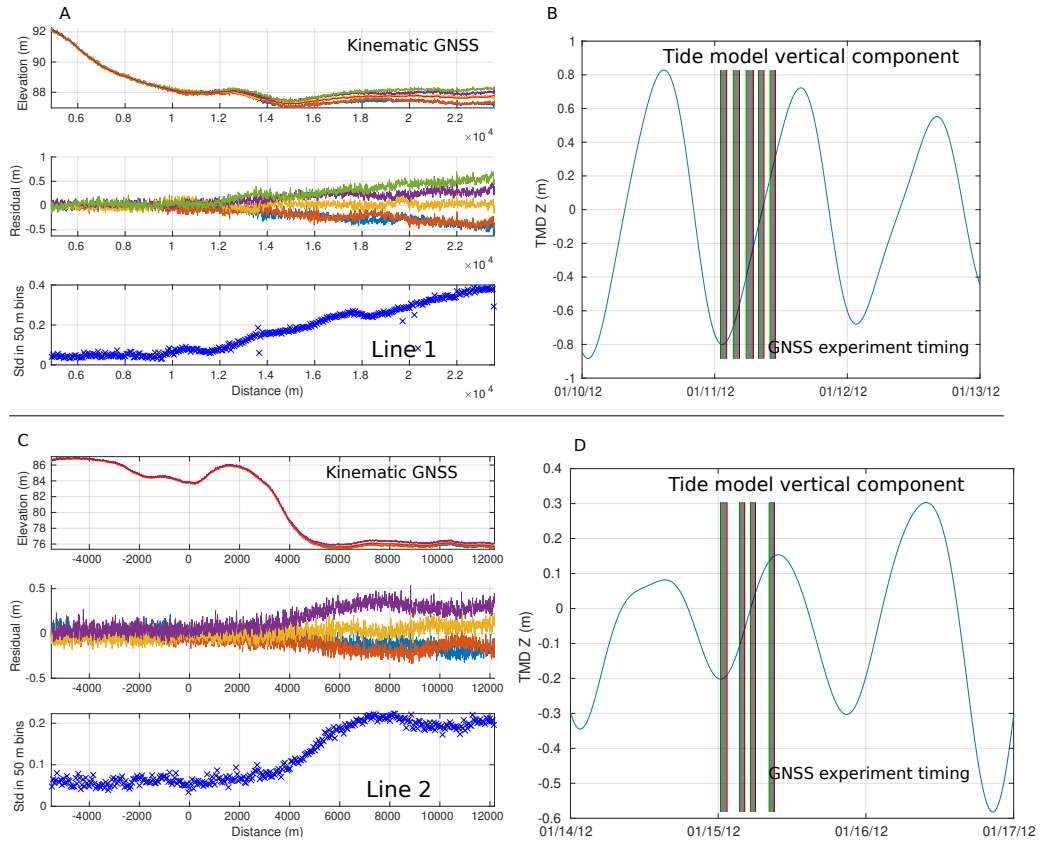


Figure 12: Repeat kinematic profiling along Lines 1 (A,B) and 2 (C,D). Panels A,C show the elevation (top), residual elevation after removal of a best-fitting spline (middle), and standard deviation of residual elevation in 50 m spatial bins (bottom). Panels B,D show the timing of the GNSS profiles overlain on vertical elevation component from Padman and Erofeeva's (2005) Tide Model Driver.